

Topological Crystalline Kondo Insulator in Mixed Valence Ytterbium Borides

Hongming Weng,^{1,2} Jianzhou Zhao,¹ Zhijun Wang,¹ Zhong Fang,^{1,2} and Xi Dai^{1,2}

¹*Beijing National Laboratory for Condensed Matter Physics, and Institute of Physics,
Chinese Academy of Sciences, Beijing 100190, China*

²*Collaborative Innovation Center of Quantum Matter, Beijing 100190, China*

(Received 13 September 2013; published 7 January 2014)

The electronic structures of two mixed valence insulators YbB_6 and YbB_{12} are studied by using the local density approximation supplemented with the Gutzwiller method and dynamic mean field theory. YbB_6 is found to be a moderately correlated Z_2 topological insulator, similar to SmB_6 but having much larger bulk band gap. Notably, YbB_{12} is revealed to be in a new novel quantum state, strongly correlated topological crystalline Kondo insulator, which is characterized by its nonzero mirror Chern number. The surface calculations find an odd (three) and an even (four) number of Dirac cones for YbB_6 and YbB_{12} , respectively.

DOI: 10.1103/PhysRevLett.112.016403

PACS numbers: 71.20.-b, 71.28.+d, 73.20.-r

Topological insulators (TIs) [1,2] have been extensively studied, but mostly for the s and p orbital systems, such as HgTe [3–5], and Bi_2Se_3 family compounds [6–8], which are free of strong correlation effects. In the presence of strong electron interactions, very fruitful topological phases can be expected, such as the topological Mott [9] or Kondo [10–12] insulators, topological superconductors [2], and fractional TI [13–15]. To pursue these exotic phases, however, an important and necessary step is to find suitable compounds, which are strongly correlated (presumably in d and f orbital systems) and topologically nontrivial. Studies on such systems are challenging both theoretically and experimentally. Nevertheless, the mixed valence phenomenon provides an important way towards this direction [12,16–18]. For instance, in rare-earth mixed valence compounds, the band inversion naturally happens between the correlated $4f$ and $5d$ states, which may lead to correlated topological phases. SmB_6 , a typical mixed valence compound, has been proposed theoretically as a “topological Kondo insulator” [10–12], and recently has been supported by transport [19–22], photo emission [23–25] and STM [26] experiments. Here the highly dispersive $5d$ conduction band intersects with the $4f$ energy levels, leading to electron transfer and strong quantum fluctuation among $4f$ atomic configurations [17]. At sufficiently low temperature, the hybridization between $4f$ orbitals and $5d$ bands will be established, resulting in the formation of “heavy fermion” bands, whose nontrivial Z_2 topological index [1,2] can be determined by the single particle Green’s function at zero frequency [27,28].

In the present Letter, we will focus on another family of binary mixed valence compounds, ytterbium borides, and propose that various correlated topological phases, in particular a new topological crystalline Kondo insulator [29–31], can be realized. Among the four typical compounds, YbB_4 , YbB_6 , YbB_{12} , and YbB_{66} , the Yb ions in YbB_4 and YbB_{66} are $2+$ or $3+$ respectively, while both the XPS and XAS data suggest that the valence of Yb in

YbB_6 and YbB_{12} is around 2.2 [32] and 2.8 [33–36], respectively, indicating the mixed valence nature. As we have proposed in Ref. [12], the local density approximation (LDA) combined with the Gutzwiller density functional theory [37] is a powerful tool to compute the ground state and the quasi-particle spectrum of such correlated systems. Using this method, we find that (1) YbB_6 is a correlated Z_2 topological insulator similar to SmB_6 but with a much larger band gap (31 vs 10 meV), and (2) YbB_{12} is a new topological crystalline Kondo insulator [29,30,38], which can be characterized by the nontrivial mirror Chern number, and shows an even number of Dirac cones on its surface.

As shown in Fig. 1, YbB_6 has the CsCl-type structure, the same as SmB_6 , with the Yb and B_6 octahedral cluster occupying the Cs and Cl site, respectively, while YbB_{12} takes the NaCl-type structure with the Yb and B_{12} cubo-octahedral cluster replacing the Na and Cl ions, respectively. The LDA part of the calculations has been done by the full potential linearized augmented plane wave method implemented in the WIEN2k package [39]. A regular mesh of $12 \times 12 \times 12$ k points is used, and the muffin-tin radii (R_{MT}) of Yb and B atoms are taken as 2.50 and 1.57 bohr. The plane-wave cutoff K_{\max} is given by $R_{MT}K_{\max} = 7.0$. The spin-orbit coupling (SOC) is included self-consistently in all calculations.

The LDA band structures, shown in Figs. 2(a) and 2(b), suggest that the major features are very similar to SmB_6 . First, the Yb- $4f$ orbitals, which split into the $j = 5/2$ and $j = 7/2$ manifolds due to the SOC, form two sets of narrow bands with the former fully occupied and the later near the Fermi level (in SmB_6 , the $j = 7/2$ manifolds are completely empty, and $j = 5/2$ states are close to the Fermi level). Second, the low energy band structure is semiconducting with a minimum gap of about 29 meV along the X - M path in YbB_6 , and a nearly zero indirect gap for YbB_{12} . Third, there are clear band inversion features around the X point in both systems. In YbB_6 , one $5d$ band goes below the $j = 7/2$ bands (by about

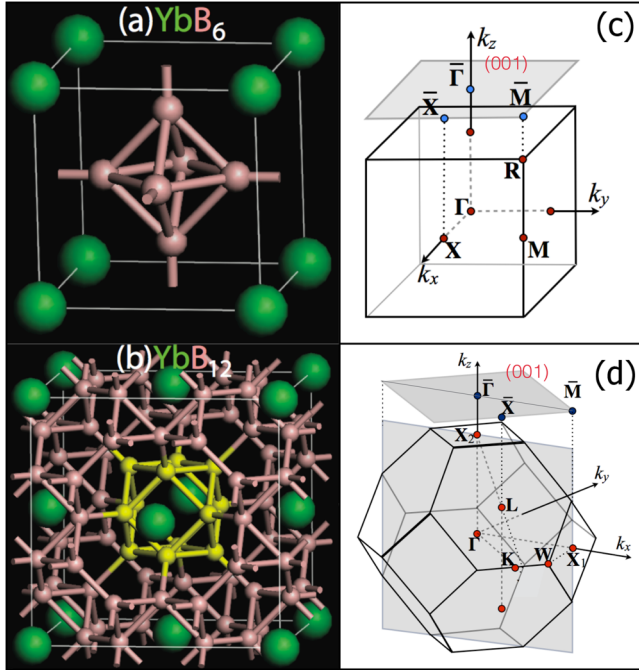


FIG. 1 (color online). (a) The CsCl-type structure of YbB_6 with $Pm\bar{3}m$ space group, and (b) the NaCl-type structure of YbB_{12} with $Fm\bar{3}m$ space group (B_{12} cubo-octahedral cluster is highlighted). (c) and (d) are the corresponding bulk and surface Brillouin zones.

1.0 eV), which reduces the occupation number n_f of the $4f$ states to be around 13.58 (resulting in the Yb valence of +2.42). What is qualitatively different in YbB_{12} is that there are two $5d$ bands (strongly hybridized with $B-2s$ and $-2p$ bands) sinking down below the $j = 7/2$ states (by about 0.8 eV), and n_f is further reduced to be 13.31, leading to the Yb valence being +2.69. We noticed that the shortest Yb-B bond length in YbB_{12} (2.277 Å) is much shorter than that in YbB_6 (by about 0.772 Å), the enhanced $5d-2p$ hybridization in YbB_{12} therefore pushes one more $5d$ state down to be lower than the $4f$ states at X point. As has been discussed in SmB_6 [12], the hybridization between the $5d$ and $4f$ states will open up a gap, and generate the semiconducting behavior. Since the $5d$ and the $4f$ states have opposite parity at the X point and there are three X points in the whole BZ, the band inversion in YbB_6 happens three (odd) times, which leads to a nontrivial TI with the Z_2 indices given as (1; 111) [40,41]. While for YbB_{12} , the band inversion happens twice at each X point, which generates totally six (even) times band inversion in the whole BZ, which gives a trivial insulator in the sense of Z_2 .

Because of the partially filled $4f$ states near the Fermi level, the on-site interactions among the f electrons are expected to play important roles, which can be captured by the LDA + Gutzwiller method [12,37]. For both systems, we take the Hubbard interaction U of 6.0 eV and

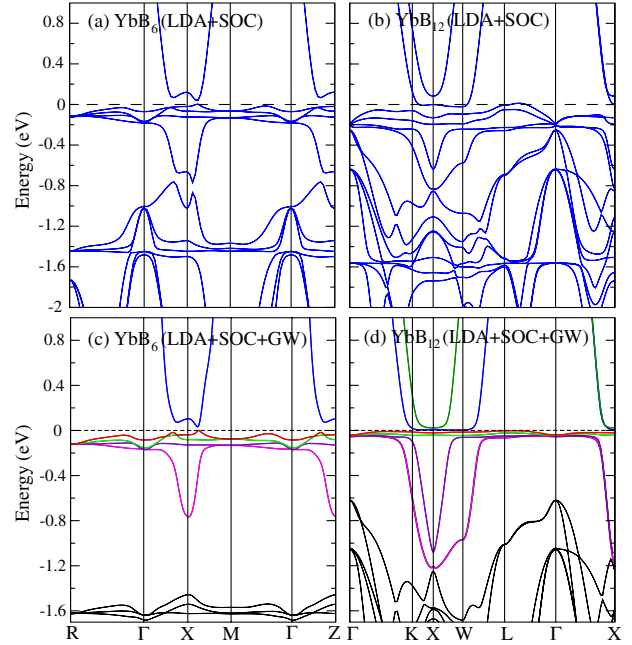


FIG. 2 (color online). The band structure of (a) YbB_6 and (b) YbB_{12} obtained from LDA + SOC calculations. (c) and (d) are their quasiparticle band structures calculated from LDA + SOC + Gutzwiller with $U = 6.0$ eV.

neglect the Hund's coupling J . From the calculated results [shown in Figs. 2(c) and 2(d)], we find three major modifications coming from the correlation effects. First, the $4f$ occupation number is further pushed towards its integer limit, namely towards $n_f \sim 13.0$ for YbB_{12} and $n_f \sim 14.0$ for YbB_6 , respectively, being in better agreement with the experimental data (see Table I). This is simply due to the fact that the strong Coulomb interactions tend to suppress the charge fluctuation among different atomic configurations. Second, we find the renormalization of the $4f$ quasiparticle bands, and the behaviors of YbB_6 and YbB_{12} are quite different. The quasiparticle weight z is 0.87 for YbB_6 but reaches very low 0.28 for YbB_{12} , indicating that the former is an intermediately correlated

TABLE I. The products of parity eigenvalues of the occupied states for TRIM points, Γ , X , R , and M for YbB_6 and Γ , X , L , and L for YbB_{12} in the BZ. n_f is the occupation number of $4f$ orbitals by LDA + Gutzwiller, compared with LDA results in the brackets and the experimental one n_f^{exp} . And z is the quasiparticle weight obtained by the LDA + Gutzwiller method.

	Γ	$3X$	$3M(L)$	$R(L)$	n_f^{exp}	n_f^{exp}	z
YbB_6	+	-	+	+	13.80(13.58)	13.8 ^a	0.87
YbB_{12}	+	+	+	+	13.11(13.31)	13.14 ^b , 13.12 ^c	0.28

^aRef. [32].

^bRef. [35].

^cRef. [36].

insulator while the latter is very close to the strong coupling description, the Kondo insulator. Since the same interaction parameters are used for both materials, the big difference in z is due to the different $4f$ occupations n_f . Third, we find that the hybridization gap between $4f$ and itinerant $5d$ bands is slightly enlarged to be 31 meV in YbB_6 and 6 meV in YbB_{12} , being much closer to the experimental values [42–44]. The parity analysis is still applicable for the quasiparticle bands obtained by the LDA + Gutzwiller method [12,27,28], and the results listed in Table I conclude that Z_2 indices stay unchanged after including the correlation effects for both materials.

One of the major differences between the Kondo insulator and band insulator is the temperature dependence of the electronic structure. For a typical band insulator, the band picture is applicable for almost all of the temperature range and the rigid band approximation is usually adopted, while for a Kondo insulator, the coherent hybridization between the localized f orbitals and the conduction bands (leading to insulating behavior) only occurs below

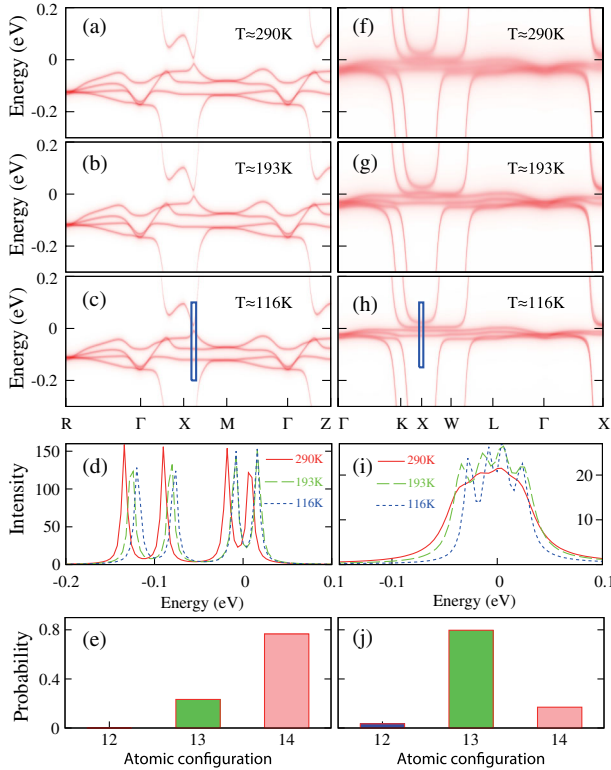


FIG. 3 (color online). The momentum-resolved spectral function $A_k(\omega)$ of YbB_6 (a)–(c) and YbB_{12} (e)–(g) at different temperatures ($T \approx 290$ K, 193 K, 116 K from top to bottom). (d) YbB_6 spectral function $A(\omega)$ at the k point with the minimum gap as indicated in (c) with $T \approx 290$ K (red), 193 K (green), 116 K (blue). (i) YbB_{12} spectral function $A(\omega)$ at the X point, as indicated in (h), with $T \approx 290$ K (red), 193 K (green), 116 K (blue). (e) and (j) are the probability of atomic eigenstates with occupation number $N_f = 12, 13, 14$ obtained by the LDA + DMFT method for YbB_6 and YbB_{12} at $T \approx 116$ K, respectively.

the Kondo temperature, which has been found to be around 220 K for YbB_{12} [35]. In order to calculate the electronic structure at finite temperature, we further apply the LDA + DMFT (dynamical mean field theory) method [45,46] to both materials. We use the continuous time quantum Monte Carlo method based on the hybridization expansion [47] for the impurity solver of DMFT, and take the same interaction parameters. The electronic spectral functions (shown in Fig. 3) obtained by the maximum entropy method [48] suggest that the two materials behave quite differently. At low temperature ($T = 116$ K), the spectral functions for both materials are in good agreement with the LDA + Gutzwiller results (plotted in Fig. 2). At 290 K, however, the spectral function of YbB_{12} is significantly smeared out, while that of YbB_6 still stays unchanged, indicating that the rigid band picture is applicable to YbB_6 but broken down for YbB_{12} , which can be viewed as a Kondo Insulator with Kondo temperature around 200 K.

The surface states (SSs) for YbB_6 and YbB_{12} (shown in Fig. 4) are obtained by using the Green’s function method based on the tight-binding model constructed from the maximally localized Wannier functions. The correlation corrections from the Gutzwiller approximation are included. For YbB_6 , the SS on the (001) surface is very similar to that of SmB_6 [12], which contains three surface Dirac cones located at $\bar{\Gamma}$ and two \bar{X} points; for its (111) surface we also find three Dirac cones located at \bar{M} , which are symmetric due to the threefold rotation along the [111]

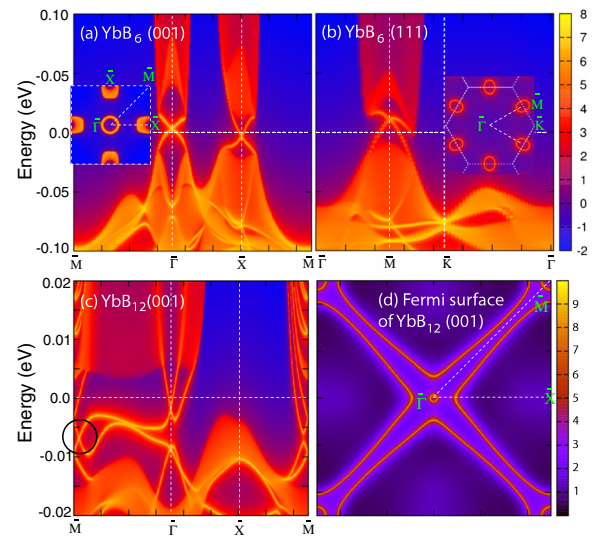


FIG. 4 (color online). The surface states (SSs) of YbB_6 for its (a) (001) and (b) (111) surface from LDA + Gutzwiller calculation. Insets are the Fermi surfaces with chemical potential 5 meV above and below the Dirac point at $\bar{\Gamma}$ drawn for (001) and (111) SSs, respectively. (c) SS of YbB_{12} (001) surface from LDA + Gutzwiller calculation and (d) its Fermi surface at Fermi level. The Dirac cone due to nonzero MCN is indicated by a circle in (c).

axis. Although YbB_{12} is topologically trivial in the sense of Z_2 , the band inversion feature around the X points generates SSs as well, which are shown in Figs. 4(c) and 4(d). Unlike YbB_6 , whose SS has odd number of Dirac points, the SS of YbB_{12} contains four Dirac points on the (001) surfaces (near the \bar{M} point along the \bar{M} to $\bar{\Gamma}$ direction), indicating that it is a topological crystalline insulator similar to SnTe [29,30,49,50]. The even number of Dirac points are protected by the reflection symmetry respect to the (100) or (010) planes [i.e., the $\Gamma X_1 X_2$ plane in Fig. 1(d)], and is the consequence of the nonzero “mirror Chern number” (MCN) within such planes, which can be defined as the Chern number of half of the occupied states (distinguished by the different eigenvalues of mirror symmetry) [29,30]. We apply the Wilson loop method introduced in Ref. [51] to calculate the MCN of YbB_{12} , and get $\text{MCN} = 2$ for the $\Gamma X_1 X_2$ plane, which is consistent with the SS behavior observed on (001) surface. In fact, the nonzero MCN obtained for the (100) mirror plane implies the appearance of SS on any surface with index $(0nm)$. Unlike the situation in SnTe , however, here the possible topological SS can appear only below the Kondo temperature, when the local $4f$ moments are effectively screened by the conduction bands and the heavy quasiparticles appear. Therefore, the nonzero MCN in YbB_{12} indicates that the ground state of YbB_{12} is a new topological crystalline Kondo insulator [31].

In summary, we have applied the LDA + Gutzwiller and LDA + DMFT methods to study the possible correlated topological phases in two mixed valence Yb compounds, YbB_6 and YbB_{12} . Our results verify that YbB_6 is a moderately correlated Z_2 topological insulator, while YbB_{12} is a strongly correlated topological crystalline Kondo insulator with $\text{MCN} = 2$.

This work was supported by the NSF of China and by the 973 program of China (No. 2011CBA00108 and No. 2013CBP21700). We acknowledge the helpful discussions with Professor P. Coleman, Professor Kai Sun, and Professor Yulin Chen.

[1] M. Z. Hasan and C. L. Kane, *Rev. Mod. Phys.* **82**, 3045 (2010).
 [2] X. L. Qi and S. C. Zhang, *Rev. Mod. Phys.* **83**, 1057 (2011).
 [3] B. A. Bernevig, T. L. Hughes, and S. C. Zhang, *Science* **314**, 1757 (2006).
 [4] M. König, S. Wiedmann, C. Brüne, A. Roth, H. Buhmann, L. W. Molenkamp, X.-L. Qi, and S.-C. Zhang, *Science* **318**, 766 (2007).
 [5] X. Dai, T. L. Hughes, X.-L. Qi, Z. Fang, and S.-C. Zhang, *Phys. Rev. B* **77**, 125319 (2008).
 [6] H. Zhang, C.-X. Liu, X.-L. Qi, X. Dai, Z. Fang, and S.-C. Zhang, *Nat. Phys.* **5**, 438 (2009).
 [7] Y. Xia *et al.*, *Nat. Phys.* **5**, 398 (2009).
 [8] Y. L. Chen *et al.*, *Science* **325**, 178 (2009).
 [9] D. Pesin and L. Balents, *Nat. Phys.* **6**, 376 (2010).

[10] M. Dzero, K. Sun, V. Galitski, and P. Coleman, *Phys. Rev. Lett.* **104**, 106408 (2010).
 [11] M. Dzero, K. Sun, P. Coleman, and V. Galitski, *Phys. Rev. B* **85**, 045130 (2012).
 [12] F. Lu, J. Z. Zhao, H. Weng, Z. Fang, and X. Dai, *Phys. Rev. Lett.* **110**, 096401 (2013).
 [13] D. N. Sheng, Z.-C. Gu, K. Sun, and L. Sheng, *Nat. Commun.* **2**, 389 (2011).
 [14] N. Regnault and B. A. Bernevig, *Phys. Rev. X* **1**, 021014 (2011).
 [15] T. Neupert, L. Santos, C. Chamon, and C. Mudry, *Phys. Rev. Lett.* **106**, 236804 (2011).
 [16] R. M. Martin and J. W. Allen, *J. Appl. Phys.* **50**, 7561 (1979).
 [17] P. Coleman, *Handbook of Magnetism and Advanced Magnetic Materials* Vol. 1, (Wiley, New York, 2007).
 [18] X. Deng, K. Haule, and G. Kotliar, *Phys. Rev. Lett.* **111**, 176404 (2013).
 [19] S. Wolgast, C. Kurdak, K. Sun, J. W. Allen, D.-J. Kim, and Z. Fisk, *Phys. Rev. B* **88**, 180405(R) (2013).
 [20] D. J. Kim, S. Thomas, T. Grant, J. Botimer, Z. Fisk, and J. Xia, *Sci. Rep.* **3**, 3150 (2013).
 [21] S. Thomas, D. Kim, S. B. Chung, T. Grant, Z. Fisk, and J. Xia, *arXiv:1307.4133*.
 [22] G. Li *et al.*, *arXiv:1306.5221v1*.
 [23] M. Neupane *et al.*, *arXiv:1306.4634v1*.
 [24] J. Jiang *et al.*, *arXiv:1306.5664v1*.
 [25] N. Xu *et al.*, *Phys. Rev. B* **88**, 121102(R) (2013).
 [26] M. M. Yee, Y. He, A. Soumyanarayanan, D.-J. Kim, Z. Fisk, and J. E. Hoffman, *arXiv:1308.1085v1*.
 [27] Z. Wang, X.-L. Qi, and S.-C. Zhang, *Phys. Rev. Lett.* **105**, 256803 (2010).
 [28] Z. Wang and S.-C. Zhang, *Phys. Rev. X* **2**, 031008 (2012).
 [29] J. C. Y. Teo, L. Fu, and C. L. Kane, *Phys. Rev. B* **78**, 045426 (2008).
 [30] T. H. Hsieh, H. Lin, J. Liu, W. Duan, A. Bansil, and L. Fu, *Nat. Commun.* **3**, 982 (2012).
 [31] M.-X. Ye, J. W. Allen, and K. Sun, *arXiv:1307.7191*.
 [32] T. Nanba, M. Tomikawa, Y. Mori, N. Shino, S. Imada, S. Suga, S. Kimura, and S. Kunii, *Physica (Amsterdam)* **186–188B**, 557 (1993).
 [33] M. Kasaya, F. Iga, K. Negishi, S. Nakai, and T. Kasuya, *J. Magn. Magn. Mater.* **31–34**, 437 (1983).
 [34] M. Kasaya, F. Iga, M. Takigawa, and T. Kasuya, *J. Magn. Magn. Mater.* **47–48**, 429 (1985).
 [35] T. Susaki *et al.*, *Phys. Rev. Lett.* **77**, 4269 (1996).
 [36] Y. Takeda *et al.*, *Physica (Amsterdam)* **351B**, 286 (2004).
 [37] X. Y. Deng, L. Wang, X. Dai, and Z. Fang, *Phys. Rev. B* **79**, 075114 (2009).
 [38] R.-J. Slager, A. Mesaros, V. Juricic, and J. Zaanen, *Nat. Phys.* **9**, 98 (2013).
 [39] P. Blaha, K. Schwarz, G. K. H. Madsen, D. Kvasnicka, and J. Luitz, *WIEN2k, An Augmented Plane Wave + Local Orbitals Program for Calculating Crystal Properties* (TU Vienna, Vienna, 2001).
 [40] L. Fu, C. L. Kane, and E. Mele, *Phys. Rev. Lett.* **98**, 106803 (2007).
 [41] L. Fu and C. L. Kane, *Phys. Rev. B* **76**, 045302 (2007).

- [42] H. Werheit, T. Au, R. Schmechel, Y.B. Paderno, and E.S. Konovalova, *J. Solid State Chem.* **154**, 87 (2000).
- [43] Y. Takeda, M. Arita, M. Higashiguchi, K. Shimada, H. Namatame, M. Taniguchi, F. Iga, and T. Takabatake, *Phys. Rev. B* **73**, 033202 (2006).
- [44] T. Susaki, Y. Takeda, M. Arita, K. Mamiya, A. Fujimori, K. Shimada, H. Namatame, M. Taniguchi, N. Shimizu, and F. Iga, and T. Takabatake, *Phys. Rev. Lett.* **82**, 992 (1999).
- [45] A. Georges, W. Krauth, and M.J. Rozenberg, *Rev. Mod. Phys.* **68**, 13 (1996).
- [46] G. Kotliar, S. Y. Savrasov, K. Haule, V. S. Oudovenko, O. Parcollet, and C. Marianetti, *Rev. Mod. Phys.* **78**, 865 (2006).
- [47] E. Gull, A. J. Millis, A. I. Lichtenstein, A. N. Rubtsov, M. Troyer, and P. Werner, *Rev. Mod. Phys.* **83**, 349 (2011).
- [48] K. Haule, C.-H. Yee, and K. Kim, *Phys. Rev. B* **81**, 195107 (2010).
- [49] Y. Tanaka, Z. Ren, T. Sato, K. Nakayama, S. Souma, T. Takahashi, K. Segawa, and Y. Ando, *Nat. Phys.* **8**, 800 (2012).
- [50] P. Dziawa *et al.*, *Nat. Mater.* **11**, 1023 (2012).
- [51] R. Yu, X. L. Qi, A. Bernevig, Z. Fang, and X. Dai, *Phys. Rev. B* **84**, 075119 (2011).